International Journal of Recent Technology and Engineering (IJRTE)
ISSN: 2277-3878, Volume-8 Issue-4, November 2019

A Wireless Wearable Back Angle Measurement System for Sports and Therapeutic Applications

Ramandeep Singh Chowdhary, Mainak Basu

Abstract: ***Back angle measurement in coronal plane provides a significant insight into the condition of spinal cord for certain physical conditions. This data would especially be useful for sports and therapeutic conditions, namely for modification of playing styles, ergonomic design, treatment of back pain and many more. Such data can also be used for injury predictions in case of repeated similar lower back movements. In this communication the authors implemented a wearable wireless system which can gather the necessary data from the candidate's body which can be further used with data analytic techniques. The implemented system is based on a modular platform which uses plug and play hardware modules viz. micro-controller, accelerometer sensor, gyroscope and an RF module. A wireless node designed, which can use the sensor data to analyze lower back movement of subject's body. A hub-module is connected to the laptop at remote site for wireless data acquisition of the meaningful signals. The implemented system shows improvement in experiment error which is an advantage over similar existing systems.***

Keywords: Bio-mechanics, data analytics device, gyroscope, sport analytics, therapeutic applications, wearable sensors.

I. INTRODUCTION

The study of the different bio-mechanical motions can yield considerable information regarding the present physical condition of the body. This is especially important consideration for athletes and persons undergoing physical rehabilitation to enhance their play style or accelerate their recuperation respectively. In the human body, pelvis and spinal cord are two of the most important bone structures which operate to support the upper body weight under a variety of conditions. Improper seating arrangements, involving these bones and the associated muscles tends to lead to back-pains and injuries [1]. Discomfort levels at pelvis increases after 45 minutes, 60 minutes, 75 minutes, and 90 minutes when analyzed with the initial phase of 15 minutes in case of prolonged sitting in males [2]. Due to the importance of back angle in determination of the possibilities of back-injuries, measurement of the former is of significant importance. Some of the researchers had carried research work in developing devices and also using off the shelf devices whichcan be used for sports and therapeutic applications.

Manuscript published on November 30, 2019.
* Correspondence Author
Ramandeep Singh Chowdhar*y, School of Engineering, GD Goenka University, Sohna, Haryana, India. Email: raman85friends@gmail.com
Mainak Basu, School of Basic and Applied Science, GD Goenka University, Sohna, Haryana, India. Email: mainak.basu87@gmail.com

Kang et. al. [3] used a wearable device on the wrist with wireless reporting functionality. Bio-signals such as ECG, pulse oximetry, blood pressure, body surface temperature, and respiration rate were collected and transmitted through RF channel. Pham et. al. [4] designed a system to monitor walking style of normal walkers and people walking with front wheel. The designed system estimates complete length of one step, time taken to complete one step, speed by which step is taken, and the distance which was used for rehabilitation assessment while walking. Russell et. al. [5] in their paper had shown the use of sensory substitution for posture detection using acoustic
and temperature sensors. Laufer et. al. [6] in their research work designed a hierarchical model based on fuzzy logic concept to classify sports activity risk level using the person's status and previously analyzed medical conditions of the same person. Roy et. al. [7] used PPG signals and ANN for health monitoring application.

In previous few years, there has been an exponential growth in the applications of sensor enabled wearable devices as discussed by Kos et. al. [8]. One of the applications as discussed by Chang et. al. [9] is health monitoring. Zhang et. al. [10] have used wearable devices for human and machine interaction purposes. Chen et al. [11] in their research had explained wearable devices used as educational tools. A case study on performance evaluation and sports monitoring is discussed by Kos et al. [8] in their research article. The implemented hardware can capture motion of different limbs and joints in a human body. These calculations are based on the parameters which describe dynamics of human body i.e. displacements, velocities and accelerations as discussed by Bort et. al. [12], Novacheck et. al. [13], and Hamner et. al. [14]. In general, measurement of movement characteristics of sport's professional is done in a controlled laboratory environment which consists of physiological tests as explained
by James el. al. [15]. The major drawback in such kind of test
is the constrained laboratory surroundings which is dissimilar to the actual conditions faced by the sports professionals. Research had been performed by Othman et. al. [16] to calculate flexion angles using rotary based potentiometers at finger joints. Masdar et al. [17] have used flex sensors attached on cloth to get knee movement range. Fathi et. al. [18] performed experiments to find spine curvatures using Shimmer sensor and recorded accelerometer sensor data in X, Y, and Z directions and used Symbolic Aggregate Approximation method for posture classification. Koumantakis et. al. [19]

used smart phone application to measure sagittal lumbosacral quiet standing posture. Another exploration on motion based sensors for activity recognition was discussed by Bao et. al. [20] and Mantyjarvi et. al. [21].

They have used a methodology in which multiple sensors were used at different body locations. Bao et al. [20] used dual axis accelerometer sensor in their research and collected accelerometer data from sensors placed at different locations of human limbs (4 in nos.). Mantyjarvi et al. [21] uses 3-axis accelerometer based sensor module installed on the athlete's waist covering both extreme sides.

The designed system in this research article uses a sensor module which is used to calculate lower back deviation angles

in coronal plane. The collected data can be used for lower back posture analysis in sports and therapeutic applications. The main advantage and novelty of this system is the flexibility in selecting the type of gyroscope as all blocks are designed using plug and play design architecture. This reduces the preference of selecting off the shelf devices which lacks flexibility in design architecture and sensor selection. The gyroscope values were only used and accelerometer values were not collected as the objective of the research work was to analyze deviation angles and calculate sector span of lower back in coronal plane. The research work carried out in this paper was based on the following points: 1) categorization of subjects based on lower back deviation angle in coronal plane, 2) replacing goniometers with digital sensor node, 3) synchronization introduced for sampling data, and 4) reduced device error in measuring joint angles.

II. IMPLEMENTED SYSTEM

The design of the system is divided into four major blocks. The components are assembled on a single PCB and are categorized as: 1) sensing block; 2) processing block (i.e. CPU); 3) communication block (i.e. wireless communication using nRF24L01); and 4) power supply block. All these locks are independent of each other and follow a modular design approach. The sensor module contains a gyroscope which is integrated inside a single chip i.e. MPU6050. Data generated from MPU6050 sensor is used for calculation of deviation angles of lower back in coronal plane for athletes and patients with lower back pain. The CPU module acts as the brain of the implemented hardware and is responsible for sensor data collection and processing of data for wireless transmission. The CPU operates on 3.3V power supply and has 5V tolerable 14 I/O lines. The wireless module (nRF24L01) is embedded on the same node and is responsible for wireless transmission of data to the wireless receiver at the hub. The wireless transmission is taking place at 115200 baud rate i.e. both wireless transmitter and wireless receiver is configured at 115200 baud rate. The forth module i.e. 9V rechargeable battery is used to supply power to the wireless node. An onboard voltage regulator IC at Arduino Nano converts the 9V supply to the desired 3.3V DC supply for the CPU. This eliminates the need of wired power source and make the node handy which can be used for data collection in the field or clinics in case of patients. Necessary experimental setup is explained to validate the correctness of the implemented design in section III.

Fig. 1 shows the flowchart for wireless sensor node which explains the flow of data and processing to be done. It senses data from the gyroscope sensor and transmit it to the receiver at the remote site. It shows the complete flow of data from the

initial state of power on to the state of continuous wireless data transmission. In this at power on state, the sensor calibration is done for 5 seconds and the sensor module should be stationary for this duration. After calibration of the sensor all three values i.e Gx; Gy; Gz are collected from the sensor and then processed by the CPU to get the meaningful data. Next, if the synchronization signal is received from the hub to start packet transmission, then the data is transmitted from node to the hub at remote site using wireless transmitter module.

In this design the most important reason for induced error is sensor misalignment due to improper installation. In case of gyroscope based measurement units, misalignment error occurs due to the difference in angle between each rotational axis of gyroscope and the reference orthogonal axis frame used for the system. The main misalignment concepts which need to be considered while designing a motion based sensor module are 1) estimation of misalignment error, and 2) impact of error on system accuracy. Two more important issues in case of gyroscope based inertial measurement units are "drift" and "lag". The drift issue is handled by calibrating the gyroscope sensor in rate+angle mode. In this calibration technique the angle of the gyroscope was read first followed by reading of rate and angle both, hence the gyroscope sensor was recalibrated.

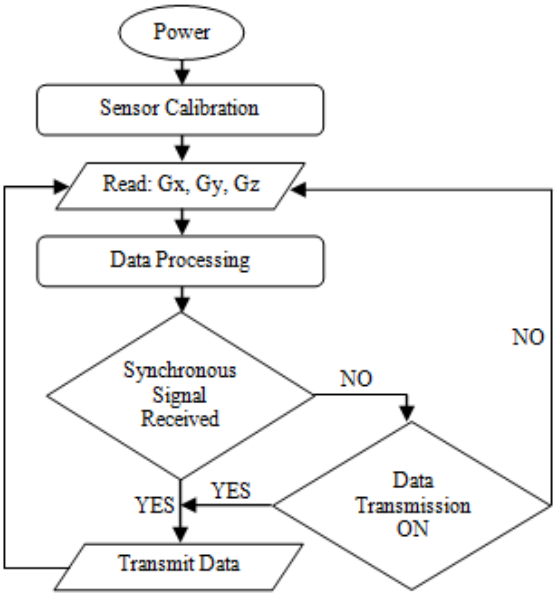

Fig. 1: Flowchart for gyroscope sensor node implementation. It process the acquired signals i.e. Gx; Gy; Gz and transmit these values to the hub for further data analytics.

The sensor was kept stationery when the calibration was going on and it takes around 5 seconds to complete the calibration process which reset the gyroscope sensor to zero. Secondly, lag introduced is negligible as data from the sensor is captured just by performing experiment for duration of 4 seconds for one subject.

III. CUSTOM DESIGNED GONIOMETER TESTBED DEVELOPMENT

An experimental setup was designed and fabricated to test the hardware devices and calculate performance metrics while performing experiments.
In this testing setup a movable acrylic rod of length 10cm and cross sectional area of 1cm^2 was mounted on a test bed base of 3mm thick acrylic sheet.

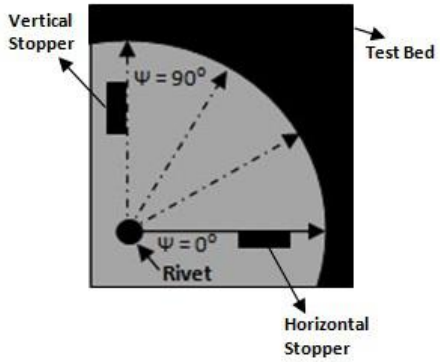

Fig. 2: Custom designed goniometer testbed for testing and validation of implemented hardware device.

The movable rod is fixed at a point on the test bed using a smooth rivet joint. The rod can move in a sector covering a total span of 90°. Two stoppers are used to mark starting and ending locations of the movable rod. The implemented hardware device having gyroscope sensor was mounted on this movable rod for testing and calculating performance metrics. Fig. 2 shows the testing and benchmarking setup which was used with gyroscope based wearable node for hardware validation. Various performance metrics was calculated using this test bed such as accuracy, error, dead time, precession, sensitivity, sampling rate and baud rate. The measured metrics are given in table II in section V. The sensor device was mounted on the movable rod at the rivet joint before performing experiments. To calculate these parameters the wireless hardware node is aligned with the axis of rotation at the rivet joint around which the hardware node is rotated. The rotation is carried from 360° to 270° and vice versa for 2 times.

A. Validation of Hardware and Experiment Process Using Custom Designed Goniometer Testbed

The experiments performed with the implemented hardware device were validated with measured values of the custom designed goniometer testbed. In the validation process the movement angle of the sensor node mounted on the testbed is measured using goniometer also. The goniometer measured value is then used for validation of observed experimental values of the movement angles. Fig. 3 is used to measure the rotation angle of NRF node around Z-axis. Stopper 1 and stopper 2 are used to restrict the movement of the acrylic rod (on which the NRF node is mounted) beyond the rotation angle span of 90° (i.e.$270° - 360°$). Using cosine rule as given in (1) ∠C (angle between side a and side b) can be calculated if sides $a, b,$ and c of the triangle are known. The proposed experiments were performed with reference side lengths as $a = 60m$ and $b = 80mm$[1]. Using these values of sides a and b mathematically calculated value of side c is $100mm$. These values represent a special case of cosine rule known as pythagoras theorem. But measured value of side c with vernier caliper is $101mm$, hence $\angle C \neq 90°$.

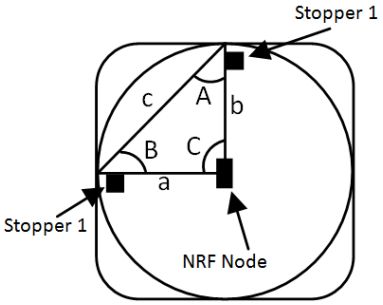

Fig. 3: Reference diagram for validation of sector angle at the time of testbed experiments: where, $a, b,$ and c are sides of the triangle in mm and $\angle A, \angle B, and\ \angle C$ are the inner angles of the triangle.

$$c^2 = a^2 + b^2 - 2ab\cos\theta \ldots\ldots (1)$$

The actual value of $\angle C$ is calculated using (1) and it's value is 91.19°. This theoretically calculated value when compared with the experimental value (RMS value of $\angle C = 91.25°$) observed from the test bed, it gives a root mean square error
(RMSE) of 0.06° in rotational angular span for NRF wireless
node around Z-axis.

IV. HARDWARE DESIGN

To overcome the disadvantages of wired and Zigbee node a wireless NRF node was designed. It consists of transceiver block based on NRF communication chip viz. nRF24L01 module working on a world wide ISM frequency band at $2.4GHz - 2.4835GHz$ and is embedded with a baseband protocol engine known as Enhanced ShockBurst™. It is an ultra low power wireless module which supports long battery life and charging is not required frequently. The power consumption of this module is very low and it just consume around $12mA$ of current during transmission.
[1]Japanese make Mitutoyo Corporation [28], vernier caliper was used for precise calculation of sides a, b, and c. Series No. 530-312, Serial No. 15117244, stainless steel hardened with least count 0.02mm.
The operating voltage range of nRF24L01 module varies from minimum of $1.9V$ to maximum of $3.6V$. The pins available on nRF24L01 module are $5V$ tolerable and it can be connected to Arduino Nano microcontroller without using any logic level converters. Some important features of nRF24L01 are that it has multiple channels (total 126 nos.) and considerably higher transfer data rate of starting from $250Kbps$ and intermediate value of $1Mbps$ and going to the maximum value of $2Mbps$. When acting as a receiver it is supported by on chip integrated channel filters. The Enhanced ShockBurst™ protocol engine has minimum of 1 byte to maximum of 32 bytes of dynamic payload, six pipes which can be used for data pipelining. This pipelining feature is known as MultiCeive™ which can receive data from 6 transmitters and can form a 1: 6 star network.

This module is smaller in size as compared to the Zigbee module as the entire module size limits to $15mm\ X\ 29mm$.

1) NRF Node Design: A wireless node was designed consisting of MPU6050 sensor which is used for data collections. Fig. 4 shows the circuit of wireless NRF node. The design was based on Arduino Nano CPU which performs calibration of MPU6050 sensor module before logging data for processing. The sensor should remain stationary for 5 seconds

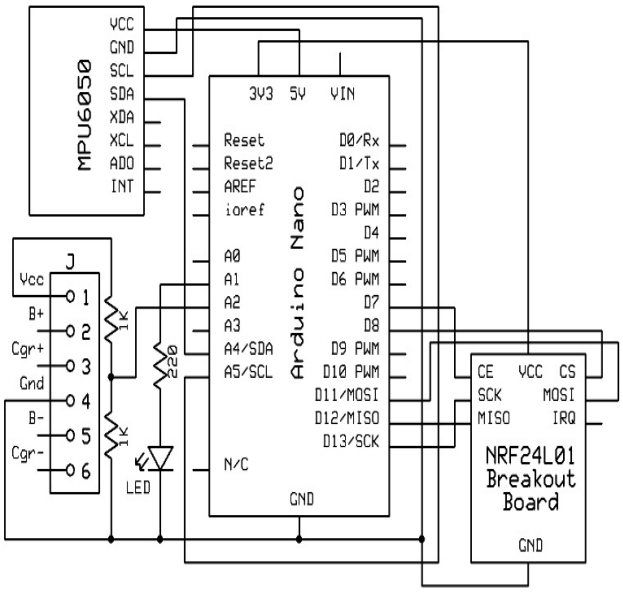

Fig. 4: Schematic diagram for wireless NRF node.

so that the CPU can perform calibration precisely. After calibration the sensor data from the MPU6050 was collected by the Arduino Nano and is processed for further transmission. The collected data is then transmitted through nRF24L01 transmitter at 115200 baud rate. The baud rate is configurable but is set at 115200 in order to perform wireless communication at high speed. The nRF24L01 module consumes $12mA$ of current while transmission. An on-board red status LED indicates calibration completion and battery status. It blinks 5 times when the calibration of MPU6050 sensor is done. A voltage divider circuit is designed to keep track of battery discharging. Status LED will be in OFF state if the battery voltage is more than the 75% of maximum value and it will be in ON state otherwise. The Node is designed using a modular approach by using plug and play interfacing modules. A double sided PCB is fabricated which can contain all the modules on a single plane along with battery for power supply. Cut out were also made in the PCB in order to mount the node on a wearable belt.

2) NRF Hub Design: Hub is used as a receiver which collects all the sensed values from the node. It is equipped with a NRF based transceiver which helps to receive and transmit wireless data. Transmission from hub is required for acknowledgment and handshaking which helps in avoiding data loss at high baud rate values. The CPU used in Hub is Arduino Nano which is connected to the laptop.

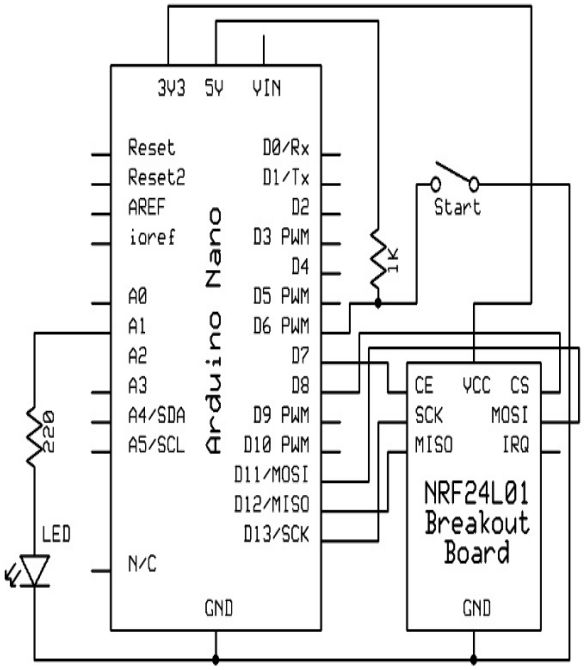

Fig. 5: Schematic diagram for wireless NRF hub.

All the received data is being used for data analytics with help of Java based GUI. The Java utility creates CSV file for multi axis sensor data coming from the node. Fig. 5 shows the schematic diagram for Hub which has a synchronous switch (denoted as "Start") for introducing synchronization in Hub- Node architecture.

V. RESULTS AND DISCUSSIONS

The implemented hardware system was used to perform experiments on the custom designed goniometer test setup (shown in fig. 2) and on 20 subjects (both male and female). Performance metrics were calculated for the implemented hardware design and are shown in table II. Following experiment was designed to be executed for calculation of performance metrics.

A. Experiments with Goniometer

Hardware Validation Experiment with custom designed goniometer: In this experiment the sensor node is mounted at the rivet joint of the custom designed goniometer and was rotated continuously at moderate speed to complete one quadrant ($360° - 270°$) and back to the $360°$ position. Fig. 6 shows the periodic motion of the wireless NRF node around z- axis (z-axis is outward of the sensor node, orthogonal to the goniometer plane) from $360° - 270° - 360°$. At some instances the angle value sensed from the MPU6050 gyroscope sensor crosses the $360°$ mark on the testbed and moves beyond it, as a result of this the sensor gives reading slightly greater than $0°$ as shown in fig. 6 by the pointer. The experiment was performed 28 times and minimum angle ($\angle min \approx 270°$) and maximum angle ($\angle max \approx 360°$) were calculated to get the angular sector span in each case. From these values the angular span was calculated as $\angle \max - \angle min$ (if the $\angle max \leq 360°$ and $\angle max \geq \angle min$) or it is equal to $360° - \angle min + \angle max$ (if $\angle max \geq 0°$ and $\angle max \leq \angle min$).

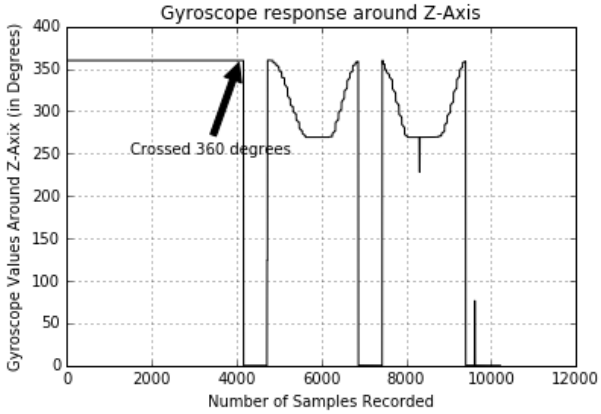

Fig. 6: Periodic motion of wireless NRF node around z-axis from 360° to 270° and back to initial position.

A comparative study for errors for different system used by various researchers is shown in table I. It showed the maximum induced error of 10° by Wen et. al. [24] and the minimum induced RMSE in 1D for lateral plane of 0.5° by Charry et. al. [27]. The implemented hardware design in this research article achieved a low RMSE value of 0.06° as shown in part A of section III.

Fig. 7 shows the distribution of angular span values of $\angle C$ for all iterations of experiments performed. It is observed from the histogram that the distribution is a Gaussian distribution and is having a peak at 90.9° which states that mode of the distribution is 90.9°. The mean, median, mode and standard deviation of the sampled data is calculated and observed as mean (μ) = 91.2°, median = 91.0°, mode = 90.9° and standard deviation (σ) = 1.2°.

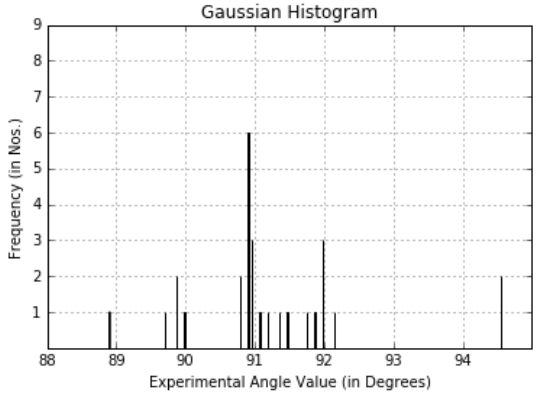

Fig. 7: Histogram of sampled data from wireless NRF node with goniometer testbed experiment for validation process.

Fig. 8 shows the box plot of the sampled data and it is observed that median = 91.0° and 50% of the values lies between 90.9° - 91.8°. The two whiskers shows the 25th percentile and 75th percentile in the box plot. 90% - 95% of the values lies between two extremes of the box plot and outliers in the sampled data are shown by '+'. This type of visualization shows the 1 dimensional way of analyzing the data.

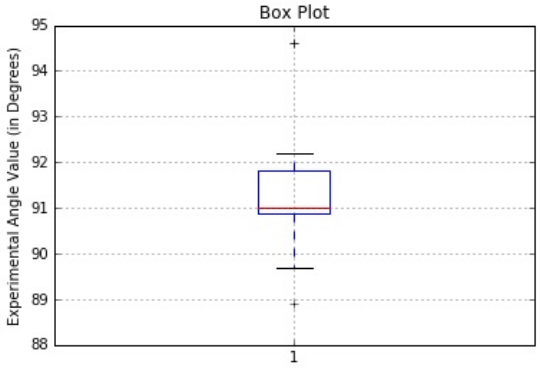

Fig. 8: Box plot of sampled data.

TABLE I: Comparison of different systems based on induced

error. (*implemented design in the present research article.)

S.	Authors	Error	Remark
1	Bonnet et al. [22]	+/-1.5°	Maximum joint error
2	Shaghayegh et al. [23]	+/-2.1°	Accuracy for knee joint angle
3	Wen et al. [24]	10°	Roll misalignment (left leg)
4	Wen et al. [24]	10°	Roll misalignment (right pocket)
5	Furukawa et al. [25]	3.1°	Vertebrae rotational error
6	Lou et al. [26]	5°	Maximum angular error
7	Charry et al. [27]	1°	RMSE for 1D in flexion plane
8	Charry et al. [27]	0.5°	RMSE for 1D in lateral plane
9	Charry et al. [27]	2.4°	RMSE for 1D in twist plane
10	Charry et al. [27]	2.1°	RMSE for 3D in flexion plane
11	Charry et al. [27]	2.4°	RMSE for 3D in lateral plane
12	Charry et al. [27]	4.6°	RMSE for 3D in twist plane
13	Masdar et al. [17]	6.92°	Average error rate
14	Present Article*	0.06°	RMSE in this research article

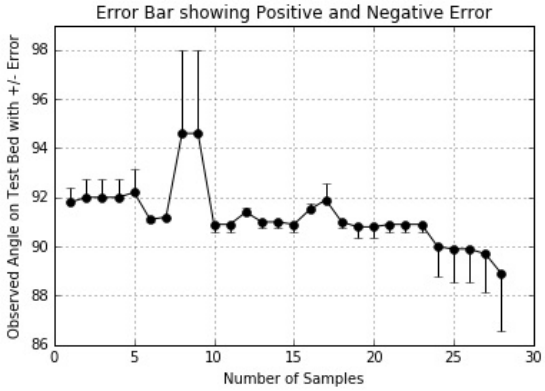

Fig. 9: Error values for all readings.

Fig. 9 shows error bars along with observed experimental values of the sector angle for all readings and it is observed that the maximum positive error is there in case of sample number 8 (S8) and sample number 9 (S9). Similarly maximum negative error is there in case of sample number 28 (S28). These samples can be removed from the data pool which was processed to get RMSE value, hence the experimental error value could be further reduced.

A comparative analysis is shown for three different datasets
in fig. 10. The periodic movement of angular motion around Z-axis from different datasets is shown using three different colors. Zero crossing, points where the angle value crosses 360° and becomes greater than 0° is shown by vertical dips in the figure. There are zero crossing points in almost all case because of misalignment error in the system as stated in section II.

From this figure it can be analyzed that all three readings shows similar pattern and it can be concluded that such similar pattern had been adopted by all experimental results for angular movement on the custom designed goniometer testbed.

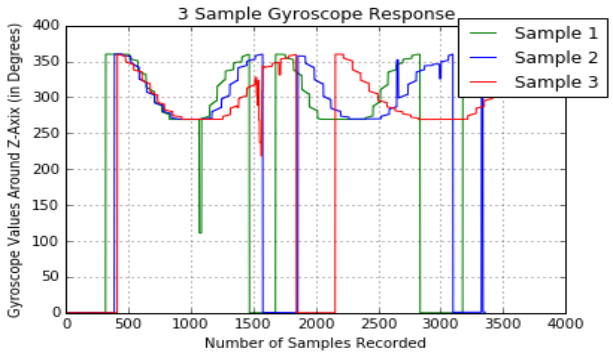

Fig. 10: Periodic motion of wireless NRF node around z-axis

from 360° to 270° and back to initial position for three data sets.

Fig. 11 shows the scatter plot resembling a linear variation of +/- error values with respect to the experimental angle value. It was observed that the majority of the sector angle were having error values of $\pm 1°$ i.e. the experimental angular span value was observed from 89° to 91°.

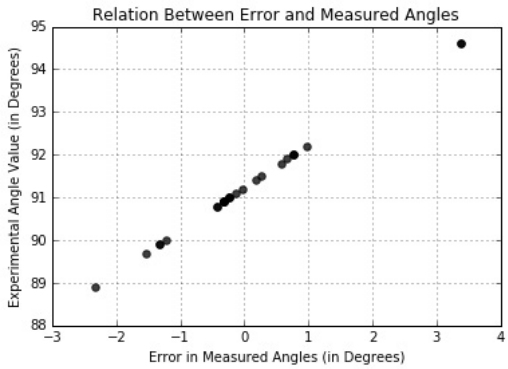

Fig. 11: Scatter plot for relationship between error in sector span angle and experimental sector span angle observed from NRF wireless node.

After performing experiment with the designed wireless hardware node different performance metrics were calculated and are given in table II. It shows that an accuracy of 82.14% is achieved with an error range of $\pm 1°$. The RMSE value is calculated from the experimental data and is equal to 0.06°. The dead time i.e. the time for which the receiver will be in a state between the two consecutive sampled values is equal to $3.3ms$. The MPU6050 sensor module and the software algorithm designed puts a restriction of 0.01° at the least count hence assigning a precision value of 0.01°. The full scale range of gyroscope was configurable and it is calibrated with the sensitivity of $\pm 250°/s$. The wireless transmission speed is selected based on baud rate of the proposed design which is assigned as 115200 at a sampling rate of 300 samples per second.

TABLE II: Performance metrics

Feature	Value	Remark
Accuracy	84.14%	Accuracy was achieved with error of +/- 1°
Error (RMSE)	0.06°	Root Mean Square Error was calculated
Dead Time	3.3ms	Time for which readings was not coming
Precision	0.01°	Least count of the designed hardware
Sensitivity	+/-250°/s	Full scale range of gyroscope in dps
Sampling Rate	300	No. of samples gathered per second
Baud Rate	115200	No. of symbols transmitted per second

B. Experiments on Subjects

The aim of the experiment is to find sector span angle of lower back of the subjects while walking. The total sector span angle is the angle formed by lower back deviation angles. As shown in fig. 12 the lower spine deviates in coronal plane towards left and right directions while walking. The total sector span angle is calculated from maximum deviation in both directions. The experiments were performed on 20 subjects (10 male and 10 female), and all were asked to walk in normal walking style for a fixed distance. The wireless sensor node was mounted on the lower back of the subject using a wearable belt. Before start of experiment the subject were asked to remain stationary for 5 seconds for sensor calibration and then after pressing the synchronization switch the wireless hub starts receiving the lower back deviation angles from the subjects while walking.

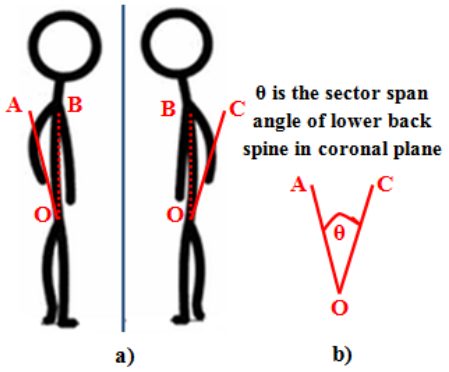

Fig. 12: a) Representation of deviation of lower spine in coronal plane while walking; b) Representation of sector span angle of lower spine while walking.

Fig. 13 shows the periodic lower back movement. It shows the deviation angles captured from the gyroscope around Z-axis (i.e. axis perpendicular to the lateral/coronal plane). The performed experiments shows that there was movement of lumbar spine in both directions around the spine. The measured values also indicate that the angular values were not same in both directions around the axis but varies on the body posture while walking. This type of study can be used as meaningful data for predicting posture correction techniques while playing and recovering from back pain problems.

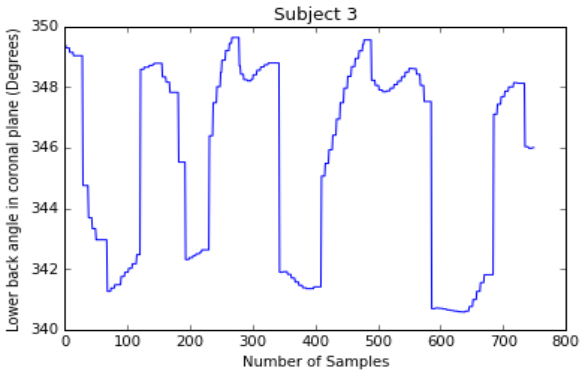

Fig. 13: Angle measurement in coronal plane.

Published By:
Blue Eyes Intelligence Engineering
and Sciences Publication (BEIESP)

Table III shows the average sector span angles of the subjects in coronal plane around Z-axis while walking among
all subjects, among male subjects, and among female subjects. It was observed that the average sector span angle for female subjects was equal to 13.2° whereas the average sector span angle for male subjects was measured as 9.3°. There was a difference of 3.9° in the average lower back sector span angles among male and female subjects. The average sector span angle of 20 subjects was coming out to be 11.25°. The maximum range of motion (in degrees) allowed across lumbar region is 19.5° (only one side) in lateral plane [29]. Thus the recorded data from 20 subjects shows that the designed hardware could be used for back angle measurement. The captured back angle data could be used for sports and therapeutic application.

TABLE III: Lower back sector span angle data measurements

Feature	Value	Remark
avg_m	9.3°	Average sector span angle for male
avg_f	13.2°	Average sector span angle for female
avg_s	11.25°	Average sector span angle for all subjects
$Angle_{Max}$	17°	Maximum sector span angle
$Angle_{Min}$	8°	Minimum sector span angle

VI. CONCLUSION

In this work the architecture, process, circuit and testbed of a wireless system was presented. The system was implemented using open source hardware and software tools which could be used for sports and therapeutic applications. The system operates in battery assisted active mode for real time data acquisition. The system could sense deviation angles in degrees around orthogonal axis. It had been seen that the accuracy of the device was 82.14% with an error of $\pm 1°$. The root mean square error was calculated to be 0.06° after performing all experiments. The device had been validated on accuracy and error and could be used to gather data for sports and therapeutic applications for body posture analysis. The experiments performed on subjects showed that the average lower back sector span angle of female subjects is higher than that of male subject while walking. The measured average lower back sector span angle for male subjects (i.e. avg_m) was 9.3° and that for female subjects (i.e. avg_f) was 13.2°. The maximum angle (i.e. $Angle_{Max}$) was 17° whereas the minimum angle (i.e. $Angle_{Min}$) was 8°.

The final design was implemented on custom design PCB using open source hardware modules. This design was based on nRF24L01 wireless module and operates in a frequency range of $2.4GHz$ to $2.4835GHz$. The system was designed for back angle measurement in wireless mode so that the measured data can be effectively used for posture correction, injury prediction and lower back analysis in sports and therapeutic applications.

REFERENCES

1. K. O'Sullivan, M. O'Keeffe, L. O'Sullivan, P. O'Sullivan, and W. Dankaerts, "The effect of dynamic sitting on the prevention and management of low back pain and low back discomfort: a systematic review", Ergonomics, vol. 55, pp. 898-908, 2012.
2. Kristina M. Gruevski, and Jack P. Callaghan, "The effect of age on invivo spine stiffness, postures and discomfort responses during prolonged sitting exposures", Ergonomics, pp. 1-33, 2019.
3. Jae Min Kang, Taiwoo Yoo, and Hee Chan Kim, "A Wrist-Worn Integrated Health Monitoring Instrument with a Tele-Reporting Device for Telemedicine and Telecare, IEEE Transactions on Instrumentation and measurement, vol. 55, no. 5, pp. 1655 - 1661, 2006.
4. Duy Duong Pham, Huu Toan Duong, and Young Soo Suh, "Walking Monitoring for Users of Standard and Front-Wheel Walkers, IEEE Transactions on Instrumentation and measurement, vol. 66, no. 12, pp. 3289 - 3298, 2006.
5. L. Russell, R. Goubran, and F. Kwamena, "Posture Detection Using Sounds and Temperature: LMS-Based Approach to Enable Sensory Substitution, IEEE Transactions on Instrumentation and measurement, vol. 67, no. 7, pp. 1543 - 1554, 2018.
6. Edit Tth-Laufer, and Annamria R. Vrkonyi-Kczy, "A Soft Computing- Based Hierarchical Sport Activity Risk Level Calculation Model for Supporting Home Exercises, IEEE Transactions on Instrumentation and measurement, vol. 63, no. 6, pp. 1400 - 1411, 2014.
7. Monalisa Singha Roy, Rajarshi Gupta, Jayanta K. Chandra, Kaushik Das Sharma, and Arunansu Talukdar, "Improving Photoplethysmographic Measurements Under Motion Artifacts Using Artificial Neural Network for Personal Healthcare, IEEE Transactions on Instrumentation and measurement, vol. 67, no. 12, pp. 2820 - 2829, 2018.
8. M. Kos, and I. Kramberger, "A Wearable Device and System for Movement and Biometric Data Acquisition for Sports Applications", IEEE Access, vol. 5, pp. 6411 6420, 2017.
9. H. C. Chang, Y. L. Hsu, S. C. Yang, J. C. Lin, and Z. H. Wu, "A Wearable Inertial Measurement System with Complementary Filter for Gait Analysis of Patients with Stroke or Parkinsons Disease", IEEE Access, vol. 4, pp. 8442-8453, 2016.
10. Y. Zhang, G. Zhou, J. Jin, Q. Zhao, X. Wang, and A. Cichocki, "Sparse Bayesian Classification of EEG for BrainComputer Interface", IEEE Transactions on Neural Networks and Learning Systems, vol. 27, pp. 2256-2267, 2016.
11. L. B. Chen, H. Y. Li, W. J. Chang, J. J. Tang and K. S. M. Li, "WristEye: Wrist-wearable Devices and a System for Supporting Elderly Computer Learners", IEEE Access, vol. 4, pp. 1454-1463, 2016.
12. J. Bort-Roig, N.D. Gilson, A. Puig-Ribera, R.S. Contreras, and S.G. Trost, "Measuring and Influencing Physical Activity with Smartphone Technology: a Systematic Review", Sports Med, vol. 44, pp. 671-686, 2014.
13. T.F. Novacheck, "The Biomechanics of Running", Gait and Posture, vol. 7, pp. 77-95, 1998.
14. S.R Hamner, and S.L. Delp, "Muscle Contributions to Fore-Aft and Vertical Body Mass Center Accelerations over a Range of Running Speeds", Journal of Biomechanics, vol. 46, pp. 780-787, 2013.
15. D.A. James, "The Application of Inertial Sensors in Elite Sports Monitoring", Moritz EF, Haake S, (eds). The Engineering of Sport 6, Vol. 3, pp. 289294, Springer; New York, 2006.
16. Azizul Othman, Norhazimi Hamzah, Zakaria Hussain, Rohaiza Baharudin, Anis Diyana Rosli, Adi Izhar Che Ani, "Design and Development of an Adjustable Angle Sensor Based on Rotary Potentiometer for Measuring Finger Flexion", 6th IEEE International Conference on Control Systems, Computing and Engineering, pp. 569-574, Penang, Malaysia, 25-27 November, 2016.
17. Aizan Masdar, B.S.K.K. Ibrahim, Dirman Hanafi, M. Mahadi Abdul Jamil, K.A.A. Rahman, "Knee Joint Angle Measurement System Using Gyroscope and Flex Sensors for Rehabilitation", Bioimedical Engineering International Conference, pp. 1-5, 2013.
18. Azin Fathi, Kevin Curran, "Detection of spine curvature using wireless sensors", Journal of King Saud University Science, vol. 29, no. 4, pp. 553-560, 2017.
19. George A. Koumantakis, Maria Nikoloudaki, Sara Thacheth, Kalliroi Zagli, Konstantina Bitrou, Andreas Nigritinos, Leon Botton, "Reliability and Validity Measurement of Sagittal Lumbosacral Quiet Standing Posture with a Smartphone Application in a Mixed Population of 183 College Students and Personnel", Journal of Hindawi Publishing Corporation Advances in Orthopedics, pp. 1-10, 2016.
20. L. Bao and S.S. Intille, "Activity Recognition from User-Annotated Acceleration Data", Ferscha A., Mattern F. (eds) Pervasive Comput., LNCS, vol. 3001, 2004.
21. J. Mantyjarvi, J. Himberg and T. Seppanen, "Recognizing human motion with multiple acceleration sensors", Proc. IEEE International Conference on Systems, Man and Cybernetics, vol. 2, pp. 747-752, 2001.

22. J. Mantyjarvi, J. Himberg and T. Seppanen, “Real-time Estimate of Body Kinematics During a Planar Squat Task Using a Single Inertial Measurement Unit”, IEEE Transactions on Biomedical Engineering, vol. 60, no. 7, pp. 747-752, 2001.
23. Shaghayegh Zihajehzadeh, Paul K. Yoon, Bong-Soo Kang, Edward J. Park, “UWB-Aided Inertial Motion Capture for Lower Body 3-D Dynamic Activity and Trajectory Tracking”, IEEE Transactions on Instrumentation and Measurement, vol. 64, no. 12, pp. 3577-3587, 2015.
24. Hsiu-Wen Chang, Jacques Georgy, Naser El-Sheimy, “Improved Cycling Navigation Using Inertial Sensors Measurements From Portable Devices With Arbitrary Orientation”, IEEE Transactions on Instrumentation and Measurement, vol. 64, no. 7, pp. 2012-2019, 2015.
25. Daisuke Furukawa, Takayuki Kitasaka, Kensaku Mori, Yasuhito Suenaga, “Spine Posture Estimation Method from Human Images Using 3D Spine Model”, Proceedings of the 17th International Conference on Pattern Recognition (ICPR04), 2004.
26. E. Lou, D. L. Hill, V. J. Raso, and N. G. Durdle, “A Posture Measurement System for the Treatment of Scoliosis”, IMTC/99. Proceedings of the 16th IEEE Instrumentation and Measurement Technology Conference, vol. 1, pp. 354-358, 1999.
27. Edgar Charry, Muhammad Umer, Simon Taylor, “Design and Validation of an Ambulatory Inertial System for 3-D Measurements of Low Back Movements”, 2011 Seventh International Conference on Intelligent Sensors, Sensor Networks and Information Processing, vol. 1, pp. 58-63, 2011.
28. Mitutoyo Corporation, http://www.mitutoyo.co.jp/eng/ products/nogisu/ hyojyun.html.
29. Donald A. Neumann, Kinesiology of the Musculoskeletal System - Foundation for Rehabilitation, Mosby Elsevier, Second Edition, pp. 359, 2010.

AUTHORS PROFILE

Ramandeep Singh Chowdhary is currently working at GD Goenka University, Haryana, India. He received his B.Tech. in Electronics and Communication in 2007 (from GGSIP University) and M.E. in Embedded Systems in 2009 (from BITS-Pilani). His specialization lies in the domain of advance embedded systems, wearable devices, embedded software development and optimization, device architecture design and related areas. He has done research work in machine learning techniques in emerging technological domains. Presently he is working on system designing and data acquisition for back angle measurement in sports and therapeutic applications. He has also contributed as key design engineer in various embedded instrumentation and robotic product development and also guided various projects in embedded system and wearable technology.

Dr. Mainak Basu is currently an Assistant Professor at the School of Basic and Applied Sciences, GD Goenka University. He received his B.Sc. (Hons.) and M.Sc. from Calcutta University in 2008 and from Jadavpur University in 2010 respectively. He was awarded his Ph.D. in Technology in 2018, in the domain of Fiber Optic sensors and instrumentation. His current focus lies in the domain of Quasi-Quantum and Neural Computer Architecture, Analog Design, Biophysics and Bioinstrumentation design. He is also actively engaged in other domains of research namely data regression and analysis using Neural Networks and design and development of robotic instrumentation.